

Effect of surface hydroxyls on DME and methanol adsorption over γ -Al₂O₃ (hkl) surfaces and solvent effects: a density functional theory study

Zhi-Jun Zuo · Pei-De Han · Jian-Shui Hu · Wei Huang

Received: 29 February 2012 / Accepted: 5 June 2012 / Published online: 5 July 2012
© Springer-Verlag 2012

Abstract Methanol and dimethyl ether (DME) adsorption over clean and hydrated γ -Al₂O₃(100) and (110) surfaces was studied by using density functional theory (DFT) combined with conductor-like solvent model (COSMO) in gas phase and liquid paraffin. On clean γ -Al₂O₃ (100) and (110) surfaces, DME and methanol preferentially interact with Al3 and Al1 of the γ -Al₂O₃(110) and (100) surfaces, respectively. On hydrated γ -Al₂O₃(100) and (110) surfaces, the OH group can influence the adsorptive behavior of DME and methanol. The Al3 and Al1 active sites of the hydrated (110) and (100) surfaces are inactivated due to hydroxyl influence, respectively. Compared to the adsorption energies of DME and methanol adsorption over the clean and hydrated (110) and (100) surfaces in gas phase and liquid paraffin, it is found that the solvent effects can slightly reduce adsorptive ability.

Keywords Adsorption · DFT · DME · γ -Al₂O₃ · Solvent effects · CH₃OH

Introduction

Dimethyl ether(DME) can be produced by methanol dehydration over a solid acid catalyst or direct synthesis from syngas over a bifunctional catalyst such as Cu/Zn/ γ -Al₂O₃. Methanol dehydration to DME is a preferable process and

more favorable in views of thermodynamics and economy [1, 2]. A lot of experimental studies on the synthesis of DME have been reported in fixed-bed reactor and slurry reactor [1–6].

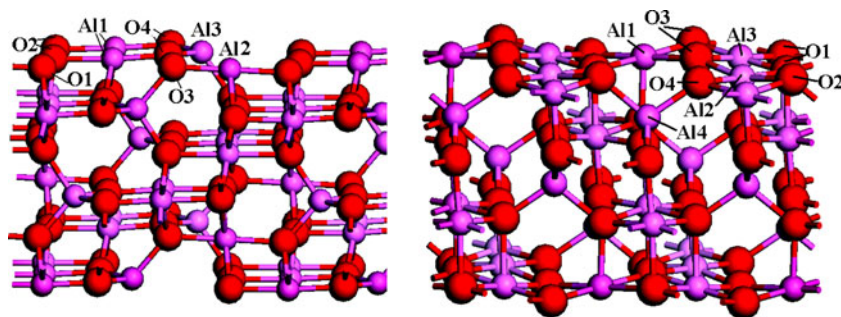
γ -Al₂O₃ has been commonly used as support in heterogeneous catalysis, such as CO₂ conversion, DME synthesis and so on. The γ -Al₂O₃ structural models based on the defective spinel model and non-spinel model have been proposed [7–10]. The defective spinel model is deduced from the existence of a spinel cubic cell, typical of MgAl₂O₄. Although the defective spinel structure is commonly used to describe the γ -Al₂O₃ structure [7, 8], the latest theoretical and experimental studies do not confirm it [9, 10]. The non-spinel model (Digne structure) is proposed on the basis of DFT study of topotactic transformation of hydrated boehmite into γ -Al₂O₃, agrees well with the experimental data [10]. Thus, we employ the non-spinel model which has been employed to construct surfaces in the previous studies [11–13].

In the paper, methanol and DME adsorption over clean γ -Al₂O₃(hkl) surface in liquid phase and gas phase are studied. Digne et al. propose the clean γ -Al₂O₃(hkl) is easily covered with water or OH group [14], Pan et al. and Zhang et al. found that the hydroxylation of the γ -Al₂O₃ supports not only influence the adsorptive behavior of CO₂, but also influence the reaction energy or even alter the pathway [12, 13]. The main byproduct of DME synthesis from methanol dehydration are water, therefore, the clean γ -Al₂O₃(hkl) is easily covered with water or OH group. Meanwhile, previous studies show that solvent effects can influence the adsorptive behavior [15, 16]. Thus, the adsorption behavior of methanol over clean and hydrated γ -Al₂O₃(hkl) surface in gas phase and liquid phase are studied. The results may be of interest to researchers attempting to investigate the reaction of methanol dehydration over γ -Al₂O₃ catalysts in bed fixed and slurry reactor.

Z.-J. Zuo · J.-S. Hu · W. Huang (✉)
Key Laboratory of Coal Science and Technology
of Ministry of Education and Shanxi Province,
Taiyuan, China
e-mail: huangwei@tyut.edu.cn

P.-D. Han
College of Materials Science and Engineering,
Taiyuan University of Technology,
Taiyuan 030024 Shanxi, China

Fig. 1 Side views of the clean γ - Al_2O_3 (110) (left) and (100) (right) surface. red: oxygen; pink: aluminum



Computational methods

The DFT calculations were performed by using the Dmol³ package in Materials Studio. The exchange-correlation energy and the potential were described by the PW91 functional [17]. Double numerical atomic orbital basis set plus polarization function (DNP) was used [18]. In order to simulate the solvent effects, the conductor-like solvent model (COSMO) implemented into Dmol³ was used [19]. COSMO is a continuum solvent model where the solute molecule forms a cavity within the dielectric continuum of permittivity, ϵ , that represents the solvent [20–22]. The charge distribution of the solute polarizes the dielectric medium. The response of the dielectric medium was described by the generation of screening (or polarization) charges on the cavity surface. The dielectric constant of liquid paraffin is considered as 2.06. We do not use the COSMO in gas phase.

Previous experimental and theoretical studies that examine the γ - Al_2O_3 surface have established that the γ - Al_2O_3 (110) and (100) surfaces were preferentially exposed [12, 23, 24]. Therefore, γ - Al_2O_3 (110) and (100) surfaces were considered here. To minimize the interaction of adsorbates of the neighboring slabs, supercells of (1×2) and (2×1) for γ - Al_2O_3 (110) and (100) surfaces were chosen respectively, which contain 24 and 16 Al_2O_3 units. The last two slabs of γ - Al_2O_3 (110) and (100) surfaces were frozen in their bulk

positions, and other slabs and adsorbates were fully relaxed. The vacuum zone between the slabs was set to 15 Å. All calculation with a k-point grid of (2×2×1) and (2×2×1) gave a numerical difference in γ - Al_2O_3 (110) and (100) surfaces energy of less than 0.005 eV.

The adsorption energy (E_{ads}) was examined by $E_{\text{ads}} = E(\text{adsorbate/slab}) - [E(\text{adsorbate}) + E(\text{slab})]$, where $E(\text{adsorbate/slab})$, $E(\text{adsorbate})$, and $E(\text{slab})$ stand for the total energy of the slab with DME or methanol over the surface, respectively. A negative corresponding to an exothermic process, indicated a stable adsorption [25].

Results and discussion

According to the coordination of the atoms of the γ - Al_2O_3 (hkl), the unsaturated Al and O atoms comprise the Lewis acid and base sites, respectively. Many studies indicate that DME synthesis from methanol occurs over the Lewis acid sites [26–28]. Thus, in this study, only adsorption over Al sites is considered.

Methanol and DME adsorption over clean γ - Al_2O_3 (hkl) surfaces

The side view of the clean γ - Al_2O_3 (110) and (100) surface is shown in Fig. 1. It can be seen that O1 and O2 atoms are three-

Fig. 2 Optimized adsorption configuration of DME and methanol over the clean γ - Al_2O_3 (110) surface in gas phase (bond distances in angstrom). (a) and (d), (b) and (e), (c) and (f): Al1, Al2 and Al3 sites. white: hydrogen; gray: carbon, and others are the same as in Fig. 1

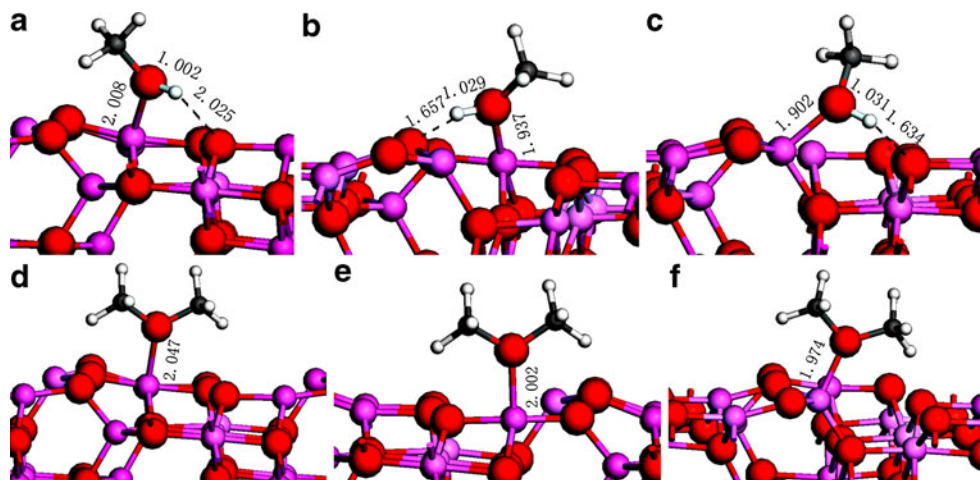
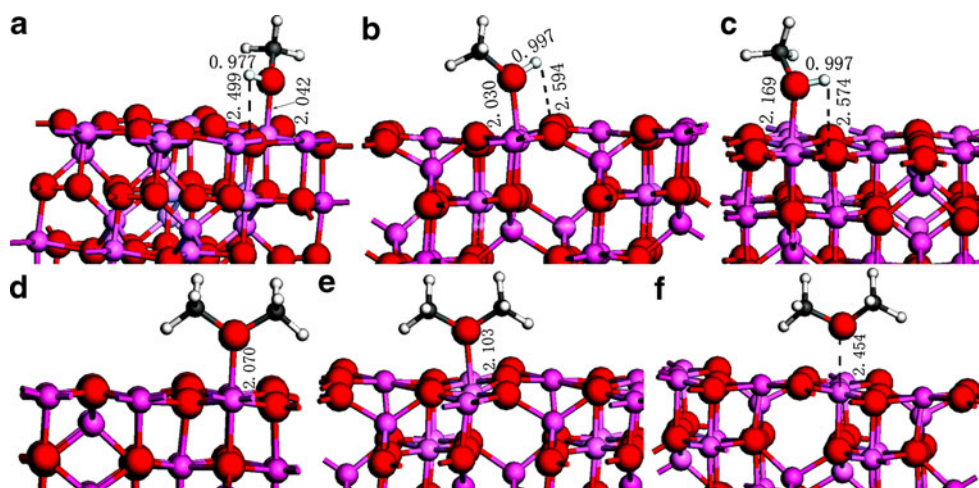


Fig. 3 Optimized adsorption configuration of DME and methanol over the clean γ - $\text{Al}_2\text{O}_3(100)$ surface in gas phase (bond distances in angstrom). (a) and (d), (b) and (e), (c) and (f): Al1, Al2 and Al3 sites. See Figs. 1 and 2 for color coding



fold coordinated on γ - Al_2O_3 (110) surface, and O3 and O4 atoms are two-fold coordinated, however, O1 and O2 atoms, O3 and O4 atoms are different in chemical environments. The (110) surface exhibits two kinds of unsaturated aluminum surface sites: 75 % of four-fold-coordinated aluminum atoms and 25 % of three-fold-coordinated aluminum. Al1 and Al2 atoms are four-fold coordinated but have difference in chemical environments, and Al3 is three-fold coordinated.

As for γ - Al_2O_3 (100) surface, it is obvious that O1 atoms are four-fold coordinated, and O2, O3 and O4 atoms are three-fold coordinated, but all atoms have a difference in chemical environments. In the case of Al atoms, Al4 is four-fold coordinated and in a position below the surface plane, therefore, it is not available for adsorption. Al1 ~ Al3 atoms are five-fold coordinated, however, Al1 ~ Al3 atoms are different in the chemical environments. Thus, we only consider DME and methanol adsorption over Al1 ~ Al3 sites.

The preferential adsorption morphologies of DME and methanol over clean γ - Al_2O_3 (110) and (100) surfaces in gas phase are shown in Figs. 2 and 3, and the corresponding adsorption energies are summarized in Table 1.

As shown in Table 1, DME and methanol adsorption over the (110) and (100) surfaces have exothermic adsorption

energies, indicating that DME and methanol adsorption over γ - Al_2O_3 surfaces are thermodynamically favored. The greater the exothermic adsorption energies, the more stable the adsorption models, therefore the thermodynamic preference of DME and methanol adsorption is the Al3 and Al1 site of γ - $\text{Al}_2\text{O}_3(110)$ and (100) surfaces, respectively.

Digne et al. have reported the energy level of the surface Lewis acid site for both the (100) and (110) surfaces, Al3 site of the (110) surface exhibits the strongest Lewis acidity, then Al2 and Al1 sites of the (110) surface, and finally Al1, Al2 and Al3 sites of the (100) surface in a decreasing sequence [14]. As given in Table 1, the stronger the Lewis acidity of the Al site, the stronger the adsorption over it. The result shows that stronger Lewis acidity is a benefit to DME and methanol adsorption. Good agreement is found with the experimental and theoretic studies of the isopropanol, CO and other adsorbates interaction with different modifications of alumina, which three-fold coordinated aluminum sites have a more pronounced Lewis acid character than four- and five-fold coordinated ones [29–31]. Compared with the adsorption energies in gas phase and liquid paraffin, the adsorption energies of those adsorbates in liquid paraffin are less negative than that of in gas phase. The trend shows that solvent effects will reduce the ability of DME and methanol adsorption over clean γ - $\text{Al}_2\text{O}_3(110)$ and (100) surfaces.

Table 1 Adsorption energies (E_{ads} , eV) of DME and methanol over the clean γ - $\text{Al}_2\text{O}_3(\text{hkl})$ surface

Sites	Gas phase		Liquid paraffin	
	$E_{\text{ads}}(\text{CH}_3\text{OH})$	$E_{\text{ads}}(\text{DME})$	$E_{\text{ads}}(\text{CH}_3\text{OH})$	$E_{\text{ads}}(\text{DME})$
(110)-Al1	-1.06	-0.93	-0.88	-0.60
(110)-Al2	-1.23	-0.94	-1.03	-0.62
(110)-Al3	-1.28	-1.04	-1.07	-0.65
(100)-Al1	-0.88	-0.87	-0.75	-0.69
(100)-Al2	-0.85	-0.84	-0.67	-0.49
(100)-Al3	-0.67	-0.61	-0.52	-0.44

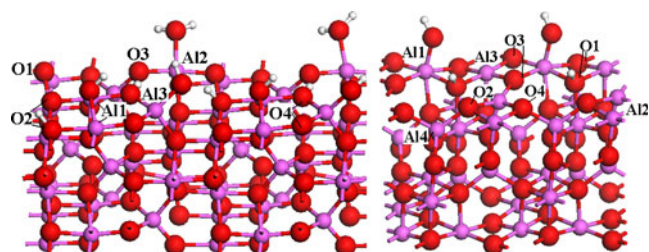


Fig. 4 Side views of the hydrated γ - $\text{Al}_2\text{O}_3(110)$ (left) and (100) (right) surface. red: oxygen; pink: aluminum. See Figs. 1 and 2 for color coding

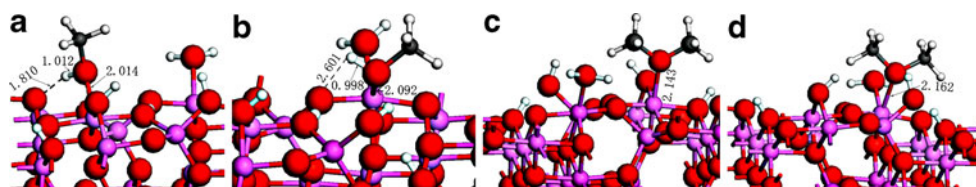


Fig. 5 Optimized adsorption configuration of DME and methanol over the hydrated γ - $\text{Al}_2\text{O}_3(110)$ surface in gas phase (bond distances in angstrom). (a) and (c), (b) and (d): Al1 and Al2 sites. See Figs. 1 and 2 for color coding

Methanol and DME adsorption over hydrated γ - Al_2O_3 (hkl) surfaces

In real reaction systems, γ - Al_2O_3 catalysts for methanol dehydration were performed in the temperature range of 230–290 °C [1–4], therefore it is necessary to consider the influence of the main product water over the properties of catalysts. The hydrated surfaces were formed by dissociative adsorption of water over the clean surfaces. The thermodynamics of hydroxylation at various OH coverages have been studied by Digne et al., who proposed that γ - Al_2O_3 (100) surface was totally dehydrated above 327 °C, whereas, in the case of the (110) surface, the OH concentration decreased from 11.8 to 3.0 OH nm⁻² between 227 and 727 °C. For the reaction temperature of methanol dehydration, the OH concentration of the (110) and (100) surfaces is 8.9 and 4.3 OH nm⁻², respectively [14].

Compared to the clean γ - Al_2O_3 (110) surface, three water molecules are necessary for OH coverage of 8.9 OH nm⁻² on the (110) surface (Fig. 4). After water adsorption, Al3 site has an adsorbed OH group, and one dissociated hydrogen group moves to surface O2; two Al1 sites share one bridge-like OH group, and one dissociated hydrogen group moves to surface O4; Al2 site has one adsorbed H₂O molecules. It can be seen that the OH group makes Al3 move to a tetrahedral position, while it is not available for adsorption, and only Al1 and Al2 sites are available for further adsorption.

Compared to the clean (100) surface, only one water molecule is necessary for OH coverage of 4.3 OH nm⁻² on the (100) surface (Fig. 4). The adsorbed water is dissociative adsorption on Al1 site while the dissociated hydrogen group moves to O1 site. Due to the influence of surface hydroxyls, Al2 and Al3 sites are available for further adsorption.

The preferential adsorption morphologies of DME and methanol over hydrated γ - Al_2O_3 (110) and (100) surfaces in gas phase are shown in Figs. 5 and 6, and the corresponding adsorption energies are summarized in Table 2. In the case of hydrated (110) surface, the adsorption energy of methanol over Al1 site in gas phase is -1.05 eV, very close to that (-1.06 eV) of the same site of the clean (110) surface. The adsorption energy of methanol over Al2 site is -1.03 eV, the adsorption ability is lower by about 0.2 eV than that of on same site of the clean surface. As for DME, the adsorption energies at Al1 and Al2 sites are -0.66 and -0.50 eV, the adsorption ability is lower by about -0.43 and -0.28 eV than that of the same sites of the clean surface, respectively.

On the hydrated (100) surface, methanol is dissociative adsorption over Al3 site in gas phase due to the influence of hydroxyl at Al1 site; On Al2 site, the adsorption energy is -0.78 eV. For DME, the adsorption energies of DME at Al2 and Al3 sites in gas phase are -0.59 and -0.83 eV, respectively. Comparing with the adsorption energies of methanol and DME over the (110) and (100) surfaces before and after hydroxylation, it is found that the adsorption order of Al2 and Al3 sites on (100), Al1 and Al2 sites on the (110) change. The reason may be hydroxyl effects the Lewis acidity when water adsorbs on Al_2O_3 surface. It should be pointed out that the Al3 and Al1 active sites of the hydrated (110) and (100) surfaces are inactivated due to hydroxyl influence respectively, and the catalysts of γ - Al_2O_3 may be deactivating. Therefore, the influence of water or hydroxyl over γ - Al_2O_3 surface in DME synthesis process need be studied in detail.

Compared with the adsorption energies in gas phase and liquid paraffin, the adsorption energies of DME and methanol in liquid paraffin are less negative than that of in gas phase. The

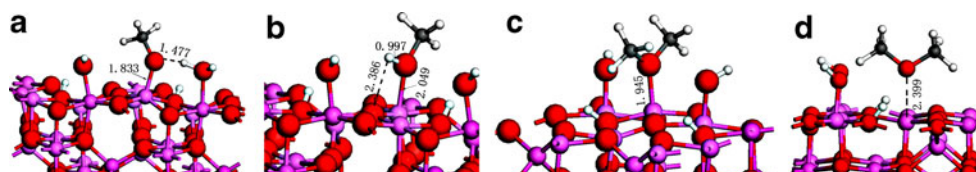


Fig. 6 Optimized adsorption configuration of DME and methanol over the hydrated γ - $\text{Al}_2\text{O}_3(100)$ surface in gas phase (bond distances in angstrom). (a) and (c), (b) and (d): Al2 and Al3 sites. See Figs. 1 and 2 for color coding

Table 2 Adsorption energies (E_{ads} , eV) of DME and methanol over the hydrated $\gamma\text{-Al}_2\text{O}_3(\text{hkl})$ surface

Sites	Gas phase		Liquid paraffin	
	$E_{\text{ads}}(\text{CH}_3\text{OH})$	$E_{\text{ads}}(\text{DME})$	$E_{\text{ads}}(\text{CH}_3\text{OH})$	$E_{\text{ads}}(\text{DME})$
(110)-Al1	-1.05	-0.66	-0.96	-0.55
(110)-Al2	-1.03	-0.50	-0.90	-0.40
(100)-Al2	-0.78	-0.59	-0.68	-0.49
(100)-Al3	— ^a	-0.83	— ^a	-0.67

^a dissociative adsorption

result shows that solvent effects can also reduce the ability of DME and methanol adsorption over $\gamma\text{-Al}_2\text{O}_3(110)$ and (100) surfaces.

Conclusions

The difference of adsorptive behavior of methanol and DME over the clean and hydrated $\gamma\text{-Al}_2\text{O}_3$ (110) and (100) surfaces in gas phase and liquid paraffin are investigated by using GGA-PW91 functional at the level of DFT. It is found that the ability of DME and methanol adsorption over the clean $\gamma\text{-Al}_2\text{O}_3$ (110) and (100) surfaces is in the order (110)-Al3 > (110)-Al2 > (110)-Al1 > (100)-Al1 > (100)-Al2 > (100)-Al3, the computed adsorption energies correlate well with the energy level of the surface Lewis sites. The OH of hydrated $\gamma\text{-Al}_2\text{O}_3$ (110) and (100) surfaces can influence the adsorption behavior of DME and methanol, and the Al3 and Al1 active sites of the hydrated (110) and (100) surfaces are inactivated due to hydroxyl influence, respectively. Compared with the adsorption energies of DME and methanol in gas phase and liquid paraffin, the result indicates that liquid paraffin destabilizes adsorbates over $\gamma\text{-Al}_2\text{O}_3$ (110) and (100) surfaces before and after hydroxylation.

Acknowledgments The authors gratefully acknowledge the financial support of this study by the National Natural Science Foundation of China (Grant No.20676087), the National Basic Research Program of China (Grant No 2011CB211709), China Postdoctoral Science Foundation Funded Project (Grant No.2012 M510784), and Shanxi Province Science Foundation for Youths (Grant No.012021005-1).

References

1. Yang RQ, Yu XC, Zhang Y, Li WZ, Tsubaki N (2008) Fuel 87:443–450
2. Kim JH, Park MJ, Kim SJ, Joo SJ, Jung KD (2004) Appl Catal A 264:37–41
3. Fan JC, Chen CQ, Zhao J, Wei Huang, Xie KC (2009) Fuel Process Technol 91:414–418
4. Gao ZH, Huang W, Yin LH, Xie KC (2009) Fuel Process Technol 90:1442–1446
5. Breman BB, Beenackers AACM, Schuurman HA, Oesterholt E (1995) Catal Today 24:5–14
6. Sherwin MB, Frank ME (1976) Hydrocarb Process 11:122–124
7. Verwey EJW (1935) Z Krist 91:317–320
8. Jennison DR, Schultz PA, Sullivan JP (2004) Phys Rev B 69:041405
9. Digne M, Sautet P, Raybaud P, Toulhoat H, Artacho E (2002) J Phys Chem B 106:5155–5162
10. Digne M, Raybaud P, Sautet P, Guillaume D, Toulhoat H (2008) J Am Chem Soc 130:11030–11039
11. Zuo ZJ, Huang W, Han PD, Gao ZH, Li Z (2011) Appl Catal A 375:181–187
12. Pan YX, Liu CJ, Ge QF (2008) Langmuir 24:12410–12419
13. Zhang RG, Wang BJ, Liu HY, Ling LX (2011) J Phys Chem C 115:19811–19818
14. Digne M, Sautet P, Raybaud P, Euzen P, Toulhoat H (2004) J Catal 226:54–68
15. Zuo ZJ, Huang W, Han PD, Li ZH (2009) J Mol Model 15:1079–1083
16. Zuo ZJ, Huang W, Han PD, Li ZH (2010) Appl Surf Sci 256:2357–2362
17. Perdew JP, Wang Y (1992) Phys Rev B 45:13244–13249
18. Hohenberg P, Kohn W (1964) Phys Rev B 136:864–871
19. Klamt A, Jonas V, Bürger T, Lohrenz JCW (1998) J Phys Chem A 102:5074–5085
20. Tomonari M, Sugino O (2007) Chem Phys Lett 437:170–175
21. Singh A, Ganguly B (2008) Mole Sim 34:973–979
22. Zuo ZJ, Sun LL, Huang W, Han PD, Li ZH (2010) Appl Catal A 375:181–187
23. Beaufils JP, Barbaux Y (1981) J Chim Phys 78:347–352
24. Nortier P, Fourre P, Saad ABM, Saur O, Lavalley JC (1990) Appl Catal 61:141–160
25. Wang SG, Liao XY, Hu J, Cao DB, Li YW, Wang JG, Jiao HJ (2007) Surf Sci 601:271–284
26. Paglia G, Buckley CE, Rohl AL, Hunter BA, Hart RD, Hanna JV, Byrne LT (2003) Phys Rev B 68:144110–144120
27. Paglia G, Rohl AL, Buckley CE, Galeet JD (2005) Phys Rev B 71:224115–224130
28. Tsyganenko AA, Mardilovich PP (1996) J Chem Soc Farad Trans 92:4843–4852
29. Maresca O, Ionescu A, Allouche A, Aycarda JP, Rajzmann M, Hutschka F (2003) J Mol Struct (THEOCHEM) 620:119–128
30. Ionescu A, Allouche A, Aycard JP, Rajzmann M (2002) J Phys Chem B 106:9359–9366
31. Feng G, Huo CF, Deng CM, Huang L, Li YW, Wang JG, Jiao HJ (2009) J Mol Catal A 304:58–64